

Low-Complexity Bandwidth-Efficient MUI/ISI-resilient CDMA based on Block-Spreading*

Shengli Zhou, Georgios B. Giannakis and Christophe Le Martret

Dept. of Elec. and Comp. Engr., Univ. of Minnesota

200 Union Street SE, Minneapolis, MN 55455

Emails: {szhou,georgios,lemartre}@ece.umn.edu

Tel: (612) 626-7781, Fax: (612) 625-4583

Abstract

A low-complexity MUI-free CDMA transceiver is developed in this paper. Relying on block spreading and zero padded transmissions, mutual orthogonality between different users' spreading codes is maintained at the receiver even after frequency selective propagation, which leads to deterministic multiuser separation with a low-complexity code-matching front-end. In addition to MUI-free reception, the proposed system guarantees channel-irrespective symbol recovery. Furthermore, it achieves high bandwidth efficiency by increasing the symbol block size. Filling the zero-gaps with known symbols allows for perfectly constant modulus transmissions. Simulation results demonstrate improved performance of the proposed system relative to competing alternatives.

1 Introduction

Relying on orthogonal spreading codes, Code Division Multiple Access (CDMA) systems allow simultaneous transmissions from multiple users over the same bandwidth. However, when the chip rate increases, the underlying multipath channel becomes frequency selective; it introduces inter chip interference (ICI) and thus destroys code orthogonality at the receiver. The latter gives rise to Multiuser Interference (MUI). To suppress MUI, various multiuser detectors are available [7], e.g., the linear decorrelator or Zero Forcing (ZF), the Minimum Mean Square Error (MMSE), as well as the nonlinear Decision Feedback (DF) and Maximum Likelihood (ML) receivers. However, these schemes require knowledge of the multipath channels for all users and/or suppress MUI statistically (except for the ZF option) even with exact Channel State Information (CSI). In addition to increased complexity that comes with multichannel estimation and multiuser detection, there even exist frequency-selective channels preventing symbol detection no matter what receiver is used [8].

To remove MUI deterministically *regardless* of the underlying FIR multipath channels, several alternatives have been proposed recently. Those include the Orthogonal Frequency Division Multiple Access (OFDMA) [5] (and generalizations [6]), where complex exponentials are utilized as information-bearing subcarriers and thus retain their shape and orthogonality when passing through multipath channels. However, when the channels have nulls (or deep fades) on some

*This research is supported by the NSF Wireless Initiative grant no. 99-79443 and the ARL grant no. DAAL01-98-Q-0648

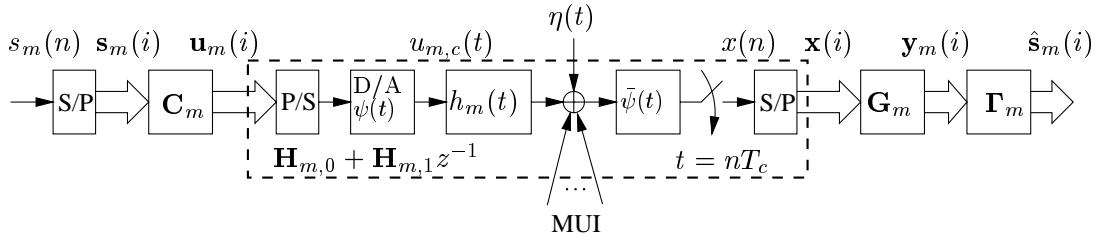


Figure 1: Continuous and discrete-time equivalent system model (m th user shown)

subcarriers, the information symbols on those subcarriers will be lost. Therefore, OFDMA-like transceivers require extra diversity (such as frequency hopping or channel coding) to ameliorate fading effects. To guarantee channel-irrespective MUI-free reception and symbol recovery, A Mutually-Orthogonal Usercode-Receiver (AMOUR) system was proposed in [2]. However, similar to other multicarrier systems, AMOUR transmissions are not Constant-Modulus (C-M) in general, even though a special code design can be C-M which will turn out to fall under the system designs developed herein. AMOUR codes are generally complex valued and bandwidth efficiency drops by 50% if real codes are to be designed from complex ones [8]. To maintain C-M at the transmitter and facilitate low-complexity receivers for MUI-free reception, the so-called shift orthogonal codes (which are not only orthogonal to each other but also to their shifted versions) were proposed in [3, 4]. However, to maintain shift orthogonality, a 50% bandwidth efficiency penalty is paid for both the real and the complex codes in [3, 4].

In this paper, we develop novel MUI-free CDMA transceivers that rely on block-spread constant-modulus transmissions. Thanks to block spreading and zero padding, mutual orthogonality between different users' codes is preserved even after multipath propagation, which allows for deterministic multiuser separation through a low-complexity code-matching front-end (Section 3). In addition to MUI-free reception, channel-irrespective symbol recovery is also guaranteed. Since the only requirement is mutual orthogonality among users' codes, the code design is very flexible and enables fast algorithms at the receiver. By increasing the symbol block size, the proposed system achieves high bandwidth efficiency. Perfectly constant modulus transmissions become available by filling the zero gaps with known symbols. Simulations are then performed in Section 4 to corroborate the improved performance of the proposed system.

2 System Modeling

The block diagram in Fig. 1 describes a CDMA system model in the downlink or uplink scenario, where only one user (the m th user out of a maximum M users) is shown. Unlike traditional spreading which is performed over a *single symbol*, we here use block spreading that operates on a *block of symbols*; in other words, the information stream of the m th user $s_m(n)$ is first parsed into K -long blocks $\mathbf{s}_m(i) := [s(iK), s(iK + 1), \dots, s(iK + K - 1)]^T$ and then block spread by a $P \times K$ spreading matrix \mathbf{C}_m to obtain the $P \times 1$ output vector $\mathbf{u}_m(i) := \mathbf{C}_m \mathbf{s}_m(i)$. After Parallel to Serial (P/S) conversion, the m th user's coded chip sequence $u_m(n)$ is pulse shaped to the corresponding continuous time signal $u_m(t)$. The latter propagates through a (possibly *unknown*) channel $h_m(t)$ and is filtered by the receive filter. Let $h_m(l)$ (with order L_m) denote the equivalent discrete time channel impulse response that includes the m th user's asynchronism in the form of delay factors as well as transmit-receive filters and multipath effects, and $\eta(n)$ be

the sampled noise. The received signal from all users at the chip rate can then be written as

$$x(n) = \sum_{m=0}^{M-1} \sum_{l=0}^{L_m} h_m(l) u_m(n-l) + \eta(n). \quad (1)$$

Similar to [6, 2, 3], we here focus on a quasi-synchronous (QS) system, where mobile users attempt to synchronize with the base-station's pilot waveform. Thus, the maximum channel order $L := \max_m L_m$ for all users can be made small (relative to the block size K) provided that we select K and the transmitted block length $P \gg L$.

The received samples $x(n)$ are serial to parallel converted to form $P \times 1$ vectors: $\mathbf{x}(i) := [x(iP), x(iP+1), \dots, x(iP+P-1)]^T$. Define the noise vector $\boldsymbol{\eta}(i) := [\eta(iP), \eta(iP+1), \dots, \eta(iP+P-1)]^T$; and, let $\mathbf{H}_{m,0}$ be the $P \times P$ lower triangular Toeplitz matrix with first column $[h_m(0), \dots, h_m(L), 0, \dots, 0]^T$, and $\mathbf{H}_{m,1}$ be the $P \times P$ upper triangular Toeplitz matrix with first row $[0, \dots, 0, h_m(L), \dots, h_m(1)]$. The Input-Output block relationship of the channels can be described by [8]:

$$\mathbf{x}(i) = \sum_{m=0}^{M-1} [\mathbf{H}_{m,0} \mathbf{C}_m \mathbf{s}_m(i) + \mathbf{H}_{m,1} \mathbf{C}_m \mathbf{s}_m(i-1)] + \boldsymbol{\eta}(i), \quad (2)$$

where the second term in the sum accounts for the Inter Block Interference (IBI).

To extract the μ -th user from $\mathbf{x}(i)$, a linear multiuser separating front-end for user μ , denoted by the matrix \mathbf{G}_μ , is applied to $\mathbf{x}(i)$. The MUI-free output is then equalized by a linear single user equalizer $\boldsymbol{\Gamma}_\mu$ as in the following:

$$\mathbf{y}_\mu(i) = \mathbf{G}_\mu \mathbf{x}(i), \quad \hat{\mathbf{s}}_\mu(i) = \boldsymbol{\Gamma}_\mu \mathbf{y}_\mu(i). \quad (3)$$

In the next section, we will design the transceiver pairs $\{\mathbf{C}_m, \mathbf{G}_m\}_{m=0}^{M-1}$, to separate the superposition of multiuser signals deterministically regardless of multipath propagation of (quasi-)synchronous transmissions through FIR channels of maximum order L .

3 Transceiver design

For each of the M users, we assign a distinct $M \times 1$ vector $\mathbf{c}_m := [c_m(0), \dots, c_m(M-1)]^T$. These vectors are selected to be mutually orthogonal which can be formally stated as a design constraint ($\delta(\cdot)$ stands for Kronecker's delta):

d1) select code-generating vectors: $\mathbf{c}_\mu^H \mathbf{c}_m = \delta(m - \mu)$, $\forall m, \mu \in [0, M-1]$.

Let \otimes denote the Kronecker's product, \mathbf{I}_{K+L} stand for the $(K+L) \times (K+L)$ identity matrix and define the $(K+L) \times K$ zero-padding (ZP) matrix $\mathbf{T}_{zp} := [\mathbf{I}_K, \mathbf{0}_{K \times L}]^T$. With these notations, we design our $P \times K$ user code matrices \mathbf{C}_m and correspondingly the $(K+L) \times P$ separating matrices \mathbf{G}_m as ($(\cdot)^H$ stands for conjugate transpose):

$$\mathbf{C}_m = \mathbf{c}_m \otimes \mathbf{T}_{zp}, \quad \mathbf{G}_m = \mathbf{c}_m^H \otimes \mathbf{I}_{K+L}, \quad (4)$$

where using the Kronecker product definition each block-spreading code (column of \mathbf{C}_m) turns out to have length $P = M(K+L)$. For the \mathbf{C}_m defined in (4), the serial version of the transmitted block $\mathbf{u}_m(i) = \mathbf{C}_m \mathbf{s}_m(i)$ is depicted in Fig. 2 (upper part). The roles of $\mathbf{s}_m(i)$ and \mathbf{c}_m are interchanged when one compares symbol spreading (lower part of Fig. 2) with block spreading

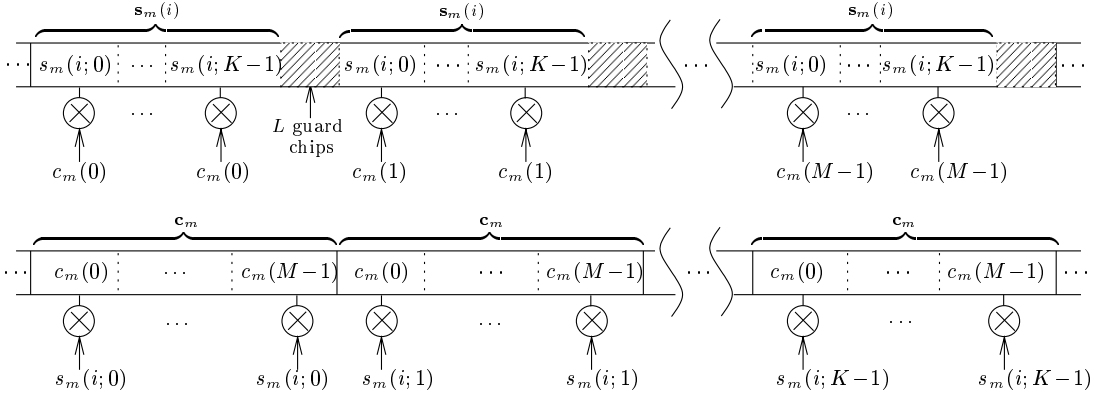


Figure 2: (Upper part) serial version of the i th transmitted block $\mathbf{u}_m(i) = \mathbf{C}_m \mathbf{s}_m(i)$ of length $M(K+L)$ versus the conventional CDMA transmission of K symbols, each spread with a short code of length M (lower part).

(upper part of Fig. 2). Indeed, the code in symbol-periodic spreading spreads each symbol, whereas the same block of symbols spreads each chip of the code in block spreading.

Note that the receive matrix \mathbf{G}_m in (4) depends only on the user's code and constitutes the code-matching user-separating front-end for user m . Next, we will show how this simple user-specific matrix \mathbf{G}_m eliminates MUI deterministically (by design) regardless of *unknown* FIR frequency-selective multipath channels.

Let $\bar{\mathbf{H}}_{m,0}$ be the $(K+L) \times (K+L)$ lower triangular Toeplitz matrix with first column $[h_m(0), \dots, h_m(L), 0, \dots, 0]^T$, $\bar{\mathbf{H}}_{m,1}$ the $(K+L) \times (K+L)$ upper triangular Toeplitz matrix with first row $[0, \dots, 0, h_m(L), \dots, h_m(1)]$, and \mathbf{J}_M an $M \times M$ shift matrix which is defined as the lower triangular Toeplitz matrix with first column $[0, 1, 0, \dots, 0]^T$. We can then split the $P \times P$ matrix $\mathbf{H}_{m,0}$ into smaller blocks and rewrite it as:

$$\mathbf{H}_{m,0} = \mathbf{I}_M \otimes \bar{\mathbf{H}}_{m,0} + \mathbf{J}_M \otimes \bar{\mathbf{H}}_{m,1}. \quad (5)$$

At this point, let us recall the identity of Kronecker products applied to matrices (with matching dimensions): $(\mathbf{A}_1 \otimes \mathbf{A}_2)(\mathbf{A}_3 \otimes \mathbf{A}_4) = (\mathbf{A}_1 \mathbf{A}_3) \otimes (\mathbf{A}_2 \mathbf{A}_4)$. Applying the latter twice, we obtain:

$$\begin{aligned} \mathbf{G}_\mu \mathbf{H}_m \mathbf{C}_m &= (\mathbf{c}_\mu^H \otimes \mathbf{I}_{K+L})(\mathbf{I}_M \otimes \bar{\mathbf{H}}_{m,0} + \mathbf{J}_M \otimes \bar{\mathbf{H}}_{m,1})(\mathbf{c}_m \otimes \mathbf{T}_{zp}) \\ &= (\mathbf{c}_\mu^H \mathbf{c}_m) \otimes (\bar{\mathbf{H}}_{m,0} \mathbf{T}_{zp}) + (\mathbf{c}_\mu^H \mathbf{J}_m \mathbf{c}_m) \otimes (\bar{\mathbf{H}}_{m,1} \mathbf{T}_{zp}) = \delta(m - \mu) \bar{\mathbf{H}}_{m,0} \mathbf{T}_{zp}, \end{aligned} \quad (6)$$

where we also used the fact that $\bar{\mathbf{H}}_{m,1} \mathbf{T}_{zp} = \mathbf{0}_{(K+L) \times (K+L)}$, which can be readily verified.

Because the last L rows of the matrix \mathbf{C}_m are zero, the IBI is eliminated since $\bar{\mathbf{H}}_{m,1} \mathbf{C}_m = \mathbf{0}_{P \times K}$. Therefore, using (2) and (6), we can express (3) as:

$$\mathbf{y}_\mu(i) = \mathbf{G}_\mu \mathbf{x}(i) = \bar{\mathbf{H}}_{\mu,0} \mathbf{T}_{zp} \mathbf{s}_\mu(i) + \mathbf{G}_\mu \boldsymbol{\eta}(i). \quad (7)$$

Equation (7) shows how the superposition of received signals from multiple users can be separated deterministically regardless of the unknown FIR multipath channels.

After MUI elimination, any single user equalizer can be applied to $\mathbf{y}_\mu(i)$ of (7) to remove the Inter Symbol Interference (ISI). Since the Toeplitz matrix $\bar{\mathbf{H}}_{\mu,0} \mathbf{T}_{zp}$ of size $(K+L) \times K$ has *always full rank*, the symbol block $\mathbf{s}_\mu(i)$ is guaranteed to be recoverable. For example, we can adopt the linear ZF equalizer given by (\dagger denotes matrix pseudo-inverse):

$$\Gamma_\mu^{zf} = (\bar{\mathbf{H}}_{\mu,0} \mathbf{T}_{zp})^\dagger, \quad (8)$$

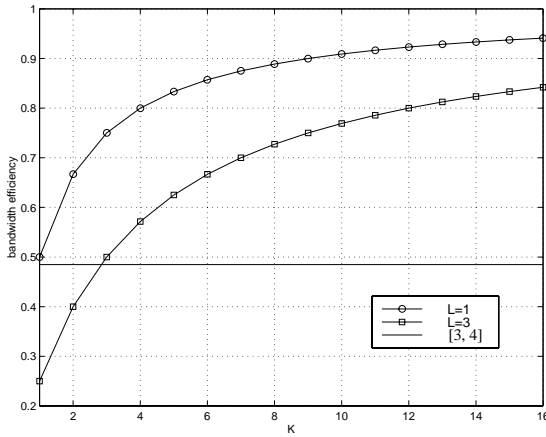


Figure 3: Bandwidth efficiency

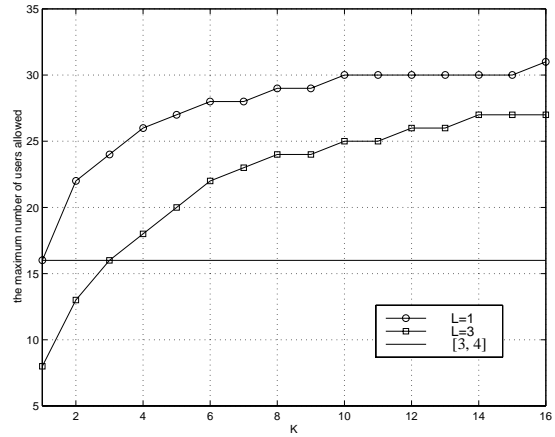


Figure 4: The maximum number of users

or, the linear MMSE, nonlinear DF and ML equalizers.

We next compare the proposed transceiver design with those in [2, 8] and [3, 4], that also achieve deterministic MUI elimination and guarantee symbol recovery; actually, they arrive at the same output [c.f. (7) with [2, eq. (19)] and [4, eq. (9)]].

3.1 Bandwidth Efficiency

Within the received $P \times 1$ block $\mathbf{x}(i)$ in (2), K information symbols are transmitted per user. The bandwidth efficiency for M users can thus be calculated as:

$$\mathcal{E}_1 = MK/[M(K + L)] = K/(K + L). \quad (9)$$

Note that the bandwidth efficiency for the AMOUR system in [2] is: $\mathcal{E}'_1 = MK/[M(K + L) + L]$. When $L \ll M(K + L)$, we obtain $\mathcal{E}_1 \approx \mathcal{E}'_1$. On the other hand, choosing $K \gg L$ enables \mathcal{E}_1 and \mathcal{E}'_1 to approach 1, which indicates that both systems have high bandwidth efficiency. In contrast, the codes in [3, 4] are designed to be shift orthogonal, which constrains their length to equal twice the number of users plus one. Thus, with our notation the bandwidth efficiency in [3, 4] is

$$\mathcal{E}_2 = MK/(2MK + K) = M/(2M + 1) < 50\%. \quad (10)$$

Selecting the information block size $K \geq L$ as in [3, 4], we find from (9) and (10) that:

$$\mathcal{E}_1 \approx \mathcal{E}'_1 \geq 50\% > \mathcal{E}_2. \quad (11)$$

Another way to look at bandwidth efficiency is to calculate the maximum number of users (with guaranteed MUI elimination and symbol recovery) that can be accommodated by the available system bandwidth. Suppose the system is allocated bandwidth W and the information rate is R_b . The spreading gain is thus $N = W/R_b$. In our system (and [2]), the spreading gain is $P/K = M(K + L)/K$ and thus the maximum number of MUI-free users is

$$M = KN/(K + L), \quad (12)$$

while the maximum number is $(N - 1)/2$ for [3, 4] ($N - 1$ should also be a power of 2).

To illustrate the difference between our system and [3, 4], we compare in Fig. 3 the corresponding bandwidth efficiencies for channels of maximum order $L = 1$ (2-rays) and $L = 3$ (4-rays) with K varying from 1 to 16. Setting the spreading gain to $N = 33$, Fig. 4 shows the maximum number of MUI-free users that are allowed. Certainly, with increasing K decoding delays increase, but our system can accommodate many more users than [3, 4].

Table 1: complexity of Multiuser Separating front-end

	single user	M users	FFT (or FWT) based algorithms
this paper	$O(M(K + L))$	$O(M^2(K + L))$	$O(M(\log_2 M)(K + L))$
[3, 4]	$O(2M(K + L))$	$O(2M^2(K + L))$	not available
[2, 8]	$O(P(K + L))$	$O(MP(K + L))$	$O(M(\log_2 M)(K + L))$

3.2 Complexity and Design Flexibility

Since MUI-free transceivers decouple MIMO transmissions into multiple parallel SISO transmissions, they have in general lower complexity than joint multiuser detectors (see, e.g., [4] for a comparison). Here we will compare the computational complexity among the three different MUI-resilient transceivers: this paper's and those in [2, 8] and [3, 4]. First, we note that all three transceivers arrive at the same single user block model (7); hence, the complexity of blind channel estimation and equalization is identical. The main difference lies in the multiuser separating front-end matrices \mathbf{G}_m . For this reason, we only concentrate on the complexity differences among the three front-ends.

For each user in our proposed transceiver, the front-end consists of $K + L$ inner products between $M \times 1$ vectors. Since each M -long correlator requires M multiplies and $M - 1$ adds, its complexity is $O(M)$. So the complexity per user is $O(M(K + L))$ and the overall complexity for all users (e.g., at the Base Station (BS) where we need to demodulate all users' information) is $O(M^2(K + L))$. With M users in [3, 4], the shift-orthogonal codes have length $2M + 1$ and subsequently each receiver needs $K + L$ inner products between $2M \times 1$ vectors after discarding 1 cyclic prefix. Therefore, each user in [3, 4] has the complexity of $O(2M(K + L))$, and the overall complexity for M users will be $O(2M^2(K + L))$.

Unlike [3, 4], where only a special class of codes with 50% bandwidth-efficiency is constructed, and different from [2], where highly-efficient codes are generally complex, the design herein is very flexible because the only requirement on our spreading codes is their mutual orthogonality. Since the design of orthogonal codes has been well developed in the literature (at least for multipath-free propagation), there are many fast algorithms available. Using such algorithms, the complexity of our transceivers can be lowered even further. For example, we can adopt IFFT or Walsh-Hadamard (W-H) codes for the code-generating vector \mathbf{c}_m in (4). Then at the BS, we can apply FFT or Fast Walsh Transform (FWT) to separate users. If the FFT is employed, the complexity for all users is $O(M(\log_2 M)(K + L))$, while the FWT is even faster than the FFT.

For each user in [2], the front-end consists of $K + L$ inner products between the $P \times 1$ received block and different Vandermonde vectors. So the complexity per user is $O(P(K + L))$ and the overall complexity for M users will be $O(MP(K + L))$. Note that AMOUR codes can also be constructed based on FFTs to reduce computational complexity. The simplest AMOUR code is proposed in [8, eq. (25)] as:

$$\mathbf{C}_m = \mathbf{f}_m \otimes \mathbf{T}_{zp}, \quad (13)$$

with \mathbf{f}_m the m th column of $M \times M$ FFT matrix. Since $\{\mathbf{f}_m\}_{m=0}^{M-1}$ satisfy d1), it is subsumed in our code designs herein and the resulting receiver has complexity $O(M(\log_2 M)(K + L))$.

For clarity, we summarize complexity requirements and comparisons with [2, 8] and [3, 4] in Table 1. With the same number of users, we infer from Table 1 that our system has less complexity than [3, 4], and the difference becomes more pronounced if special codes (e.g., W-H or FFT) are employed. Fast algorithms for the codes in [3, 4] have not been reported.

A remark is that if channel estimation is complex, or, if the channel is varying fast and channel state information (CSI) needs to be updated frequently, the complexity of the multiuser separating front-end is less instrumental in the overall receiver design.

3.3 Perfectly Constant-Modulus Transmissions

A well-known drawback of multi-carrier systems is that the transmitted signal is not of constant modulus, which imposes restrictions on the system hardware design and undesirable back-offs in the high power amplifier (HPA). Note that the system in [3, 4] has constant modulus, while our system and the FFT-based designs of [2, 8] have constant modulus except at the guard zeros. Although not a problem for the HPA, usage of guard zeros may cause on/off implementation problems in analog system designs. However, with a digital signal processing (DSP) unit and a Digital to Analog Converter (D/A) at the transmitter, inserting zeros is not a problem in e.g., software radio systems. Nevertheless, as we detail next, the proposed transmitter can also dispense with zero padding and achieve perfectly constant modulus transmissions.

With the code design in (4), the $P \times 1$ transmitted block $\mathbf{u}_m(i) = \mathbf{C}_m \mathbf{s}_m(i)$ has M zero sub-blocks of length L evenly distributed across each block. To make up for perfectly constant modulus, we fill in the zero gaps using $L \times 1$ nonzero vectors with entries drawn from the same constellation as $\mathbf{s}_m(i)$; that is, we modify the transmitter as:

$$\check{\mathbf{u}}_m(i) = \mathbf{C}_m \mathbf{s}_m(i) + \check{\mathbf{b}}_m, \quad \check{\mathbf{b}}_m := \mathbf{1}_{M \times 1} \otimes [\mathbf{0}_{K \times 1}^T, \mathbf{b}_m^T]^T \quad (14)$$

where $\mathbf{1}_{M \times 1}$ is the $M \times 1$ vector with unit entries. In this case, the modified transmitted block $\check{\mathbf{u}}_m(i)$ has perfectly C-M across the block provided that the entries of \mathbf{C}_m and $\mathbf{s}_m(i)$ have also C-M.

We next show that these filling vectors do not change our receiver design provided that the codes are selected to have zero mean. With the modified block $\check{\mathbf{u}}_m(i)$ in (14), and the original received vector $\mathbf{x}(i)$ in (2), the new received vector $\check{\mathbf{x}}(i)$ can be expressed as:

$$\check{\mathbf{x}}(i) = \mathbf{x}(i) + \sum_{m=0}^{M-1} (\mathbf{H}_{m,0} \check{\mathbf{b}}_m + \mathbf{H}_{m,1} \check{\mathbf{b}}_m). \quad (15)$$

Thus, our task is to show that $\mathbf{G}_\mu \check{\mathbf{x}}(i) = \mathbf{G}_\mu \mathbf{x}(i)$, which is equivalent to verifying that:

$$\mathbf{G}_\mu (\mathbf{H}_{m,0} + \mathbf{H}_{m,1}) \check{\mathbf{b}}_m = \mathbf{0}, \quad \forall m, \mu \in [0, M-1]. \quad (16)$$

Note that $\mathbf{H}_{m,1}$ can be expressed as $\mathbf{J}_M^{-(M-1)} \otimes \bar{\mathbf{H}}_{m,1}$, where $\mathbf{J}_M^{-(M-1)}$ is the $-(M-1)$ st power of \mathbf{J}_M , which has only a single unity entry at the top-right corner and zeros elsewhere. Introducing the matrix $\mathbf{Z}_M := \mathbf{J}_M + \mathbf{J}_M^{-(M-1)}$ that performs a cyclic shift on a vector and using the block-expression of $\mathbf{H}_{m,0}$ in (5), we then obtain:

$$\mathbf{H}_{m,0} + \mathbf{H}_{m,1} = \mathbf{I}_M \otimes \bar{\mathbf{H}}_{m,0} + \mathbf{Z}_M \otimes \bar{\mathbf{H}}_{m,1}. \quad (17)$$

With the receive matrix \mathbf{G}_μ designed as (4) and with $\check{\mathbf{b}}_m$ inserted from (14), we arrive at:

$$\begin{aligned} \mathbf{G}_\mu (\mathbf{H}_{m,0} + \mathbf{H}_{m,1}) \check{\mathbf{b}}_m &= (\mathbf{c}_\mu^H \mathbf{1}_{M \times 1}) \otimes (\bar{\mathbf{H}}_{m,0} [\mathbf{0}_{K \times 1}^T, \mathbf{b}_m^T]^T) + (\mathbf{c}_\mu^H \mathbf{Z}_M \mathbf{1}_{M \times 1}) \otimes (\bar{\mathbf{H}}_{m,1} [\mathbf{0}_{K \times 1}^T, \mathbf{b}_m^T]^T) \\ &= (\mathbf{c}_\mu^H \mathbf{1}_{M \times 1}) \otimes (\bar{\mathbf{H}}_{m,0} + \bar{\mathbf{H}}_{m,1}) [\mathbf{0}_{K \times 1}^T, \mathbf{b}_m^T]^T, \end{aligned} \quad (18)$$

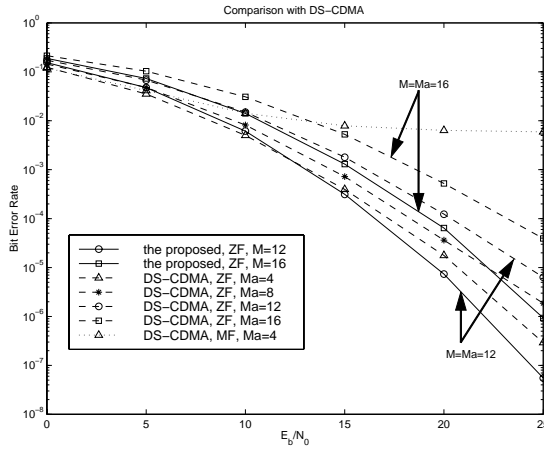


Figure 5: Comparison with DS-CDMA

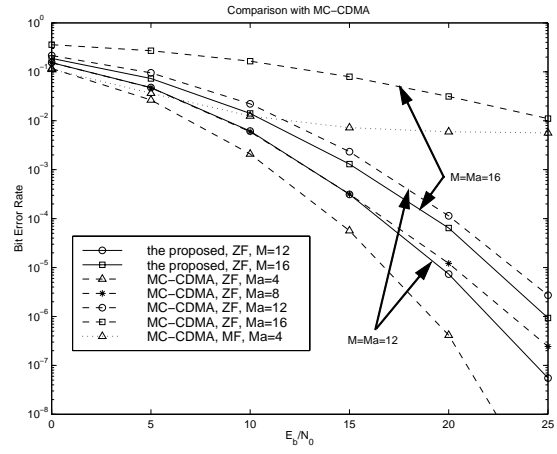


Figure 6: Comparison with MC-CDMA

where the identity $\mathbf{Z}_M \mathbf{1}_{M \times 1} = \mathbf{1}_{M \times 1}$ was used in establishing the second equality.

Therefore, (18) leads to (16) if in addition to d1) we adopt the design constraint of:

d2) balanced user codes; i.e., $\mathbf{c}_\mu^H \mathbf{1}_{M \times 1} = \mathbf{0}$, $\forall \mu \in [0, M - 1]$.

Note that d2) is not very restrictive and can be satisfied by many code designs. For instance, IFFT or W-H codes satisfy d2) after discarding only the code with all one entries. The maximum number of ZF, M , users is thus only decreased by one. Recall however that with the filling symbols in (14), we achieve a perfectly constant modulus transmission while maintaining its low-complexity MUI/ISI-resilient reception and its high bandwidth efficiency regardless of frequency-selective multipath.

The penalty with non-zero guards is a small power loss since we allocate $ML/MK = L/K$ percent of the transmit-power for the filling symbols. However, if $K \gg L$, the power loss is small and can be reduced further since the transmitters do not need to pick the same amplitude for the filling symbols as for the data symbols. If the amplitude of the filling symbols is reduced by half, the power loss decreases to one fourth of the original one. The extreme case is to insert filling symbols with zero amplitude as in (4), which incurs no power loss.

4 Simulations

To illustrate the merits of the proposed system, we here present several simulation results.

Test Case 1 (comparison with multiuser detectors): To compare the block-spread MUI-free transceivers with symbol-spread multiuser detectors, we simulate both Direct Sequence (DS) CDMA and Multi Carrier (MC) CDMA systems. The spreading gain is $N = 19$ and the channels have maximum order $L = 3$ (4-rays). Both DS-CDMA and MC-CDMA use W-H spreading codes. When only the channel of the desired user is available, the single-user matched filter (MF) receiver can be employed. The corresponding BER curve levels off and a high error floor appears due to the MUI, as shown in Figs. 5 and 6. To remove MUI, we also simulated ZF multiuser detectors for both DS-CDMA and MC-CDMA, which require knowledge of the codes and the channels of all users at the receiver-end. For the proposed transceiver, we simulated two scenarios. The first uses $K = 6$ to accommodate $M = 12$ users [c.f. (12)]. The second adopts $K = 16$, which enables MUI-free reception of $M = 16$ users. Increasing the block size K allows for more MUI-free users [c.f. (12)]; however, the decoding delay increases and the BER performance per user degrades as illustrated in Figs. 5 and 6 (it will be further elaborated in Test

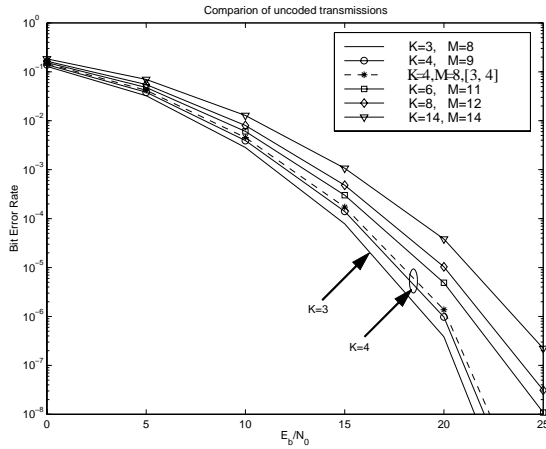


Figure 7: BER comparison with [3, 4]

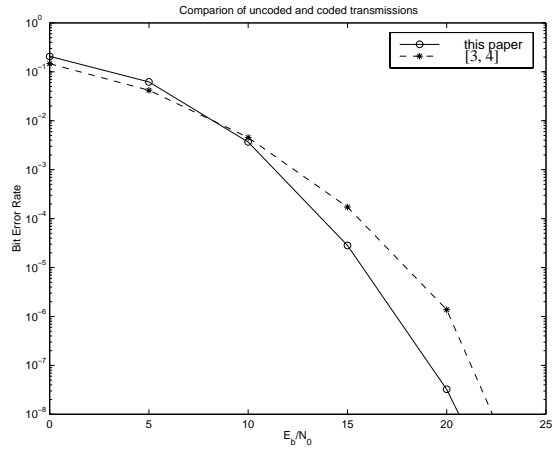


Figure 8: Coding for a fixed number of users

Case 2). Thanks to the MUI-free reception, the BER remains unchanged when the number of active users M_a ($M_a \leq M$) varies. However, for both DS-CDMA and MC-CDMA, when the number of active users M_a increases, the performance of each user degrades, as shown in Figs. 5 and 6. When the system is heavily loaded, e.g., $M_a \approx M$, the proposed MUI-free transceiver outperforms the multiuser-detectors as confirmed by Figs. 5 and 6. When the system is lightly loaded, i.e., $M_a \ll M$, the multiuser detectors could exhibit better performance since MUI is less severe in this case. A final remark here is that multiuser detectors in general require higher computational complexity for both channel estimation and equalization, as illustrated in [4].

Test Case 2 (comparison with the MUI-free transceiver of [3, 4]): To compare the proposed transceiver with those in [3, 4], we here adopt the design parameters of [3] for its shift-orthogonal transceiver: $L = 3$, $K = 4$ and $M_2 = 8$ users. The code length (spreading gain) for each user is then $N = 2M + 1 = 17$ and the block length $P_2 = NK = 68$.

Increasing K does not bring additional benefits to [3, 4]. However, K is very flexible in our system design and different trade-offs can be exploited between decoding delay, BER performance and bandwidth efficiency. To make a fair comparison, we put both transceivers with the same information rate R_b under the same system bandwidth W and thus the same spreading gain $N = W/R_b = 17$. Various system designs can be afforded by the proposed transceiver as detailed in the following:

i) We fix our system to have the same decoding delay by adopting $K = 4$. Therefore, we can afford $M_1 = 9$ users [c.f. (12)], and the block length becomes $P_1 = M_1(K + L) = 63$. Since $M_1 > M_2$ and $P_1 < P_2$, our system accommodates one more user with shorter blocks, which implies that our system has higher bandwidth efficiency than [3]: $\mathcal{E}_1 = M_1K/P_1 > \mathcal{E}_2 = M_2K/P_2$. However, since both systems reach the same block model of (7), each user has the same performance as confirmed by Fig. 7 with $K = 4$. The only difference here is that the system of [3, 4] incurs a small power loss $10 \log_{10}(17/16) = 0.26\text{dB}$ due to the cyclic prefix of length 1 (out of $N = 17$) discarded at the receiver.

ii) As confirmed by (12), the number of users increases for fixed N when K increases, which correspondingly increases the decoding delay. For example, with $K = 6, 8, 14$ we allow for 11, 12, 14 MUI-free users within a block of length $P_1 = 11 \times 9 = 99, 12 \times 11 = 132, 14 \times 17 = 238$, respectively. In addition to longer decoding delays, the BER performance degrades as shown in Fig. 7 as the maximum number of users increases. Clearly, we see the trade-offs among bandwidth efficiency, decoding delays and BER performance. We can also infer from Fig. 7 that increasing K in [3, 4] degrades system performance because it reaches the same

model (7). However, the bandwidth efficiency does not improve with K and is always limited to $MK/NK < 50\%$.

iii) We now fix the number of users to $M_1 = M_2 = 8$. Then the block length K should be chosen to satisfy: $M_1(K+L) < KN$, which requires $K > LM_1/(N - M_1)$. Therefore, we can set $K = L = 3$ here and $P_1 = 8 \times 6 = 48$, which results in smaller decoding delays and leads to better BER performance, which is shown in Fig. 7 with $K = 3$. On the other hand, we can increase the number of symbols within each data vector $\mathbf{x}(i)$ to increase throughput for a fixed number of users. For example, with a block length $P_1 = 63, 72$, we can allow for $K = 5, 6 > 4$ symbols for each of the M_1 users. However, when K and hence the symbol rate per user increases, the BER performance degrades, which can be confirmed by Fig. 7. The reason is that when K increases, the spreading gain per symbol decreases: $P_1/K = M_1(K+L)/K$ and thus the system resources are not fully utilized. To fully exploit the system bandwidth resources $P_1/K \approx N$, we can for example transmit the linearly precoded or channel coded $K' \times 1$ ($K' > K$) vector $\mathbf{s}'_m(i)$, instead of the $K \times 1$ data vector $\mathbf{s}_m(i)$, to improve the BER performance. To illustrate this point, a simple simulation is provided next.

iv) We here simulate $M_1 = M_2 = 6$ users in both systems. Since $N - 1$ should be a power of 2 and $N/2 > 6$ in [3, 4], the code length is again $N = 17$. Here, with the same $K = 4$, and $N = 17$, we use $K' = 7$ and a (7, 4) Hamming code to improve the BER performance, as confirmed by Fig. 8 where the coded BER is calculated through [1, eq. (10.67) and eq. (10.101)]. Both systems also have comparable decoding delays since $K = 4$ data symbols are transmitted over blocks of length $P_1 = 60$ and $P_2 = 68$, respectively.

References

- [1] S. Benedetto and E. Biglieri, *Principles of Digital Transmission with Wireless Applications*, Kluwer Academic/ Plenum Publishers, 1999.
- [2] G. B. Giannakis, Z. Wang, A. Scaglione, and S. Barbarossa, "AMOUR - Generalized Multicarrier Transceivers for Blind CDMA irrespective of Multipath," *IEEE Trans. on Comm.*, 2000 (to appear); see also *Proc. of GLOBECOM*, 1999, pp. 965-969.
- [3] G. Leus and M. Moonen, "MUI-Free Receiver for a Shift-Orthogonal Quasi-Synchronous DS-CDMA System Based on Block Spreading in Frequency-Selective Fading," in *Proc. of Intl. Conf. on ASSP*, June 5-9, 2000, pp. 2497-2500.
- [4] G. Leus and M. Moonen, "MUI-Free Receiver for a Synchronous DS-CDMA System Based on Block Spreading in the Presence of Frequency-Selective Fading," *IEEE Trans. on Signal Processing*, 2000 (accepted).
- [5] H. Sari and G. Karam, "Orthogonal frequency-division multiple access and its application to catv network," *Euro. Trans. on Telecom.*, pp. 507-516, Nov., 1998.
- [6] A. Scaglione, G. B. Giannakis, and S. Barbarossa, "Lagrange/Vandermonde MUI eliminating user codes for quasi-synchronous CDMA in unknown multipath," *IEEE Trans. on Signal Processing*, vol. 48, pp. 2057-2073, July 2000.
- [7] S. Verdú, *Multiuser Detection*, Cambridge Press, 1998.
- [8] Z. Wang and G. B. Giannakis, "Wireless multicarrier communications: Where Fourier meets Shannon," *IEEE Signal Processing Magazine*, pp. 29-48, May 2000.